

Charge excitations in stripe-ordered $\text{La}_{5/3}\text{Sr}_{1/3}\text{NiO}_4$ and $\text{La}_{15/8}\text{Ba}_{1/8}\text{CuO}_4$: Interpretation of the anomalous momentum transfer dependence via fluorescence interferometry

W. Schülke and C. Sternemann

Fakultät Physik/DELTA, Technische Universität Dortmund, D-44221 Dortmund, Germany

(Received 1 February 2011; revised manuscript received 29 June 2011; published 30 August 2011)

Fluorescence interferometry (FI) makes use of the temporal and spatial coherence of absorption and re-emission process in resonant inelastic x-ray scattering (RIXS), which leads to interference terms in the RIXS cross section of a group of identical, physically equivalent, and interacting atoms. These interferences contain structural information and make RIXS site selective. The basics of FI are derived within the third-order perturbation treatment of indirect RIXS. The final relations for the FI related RIXS cross section were used to interpret the unique momentum-transfer dependence of the in-gap charge excitations observed for 214-type nickelates ($\text{La}_{5/3}\text{Sr}_{1/3}\text{NiO}_4$) and cuprates ($\text{La}_{15/8}\text{Ba}_{1/8}\text{CuO}_4$). By using well-known stripe models, the momentum-transfer dependence of the corresponding indirect RIXS features is traced back to interference terms in the RIXS cross section based on the principles of FI. Thus analyzing the momentum-transfer dependence of the re-emitted radiation yields information about details of the charge stripe structure.

DOI: [10.1103/PhysRevB.84.085143](https://doi.org/10.1103/PhysRevB.84.085143)

PACS number(s): 78.70.Ck, 74.72.-h, 61.05.-a

I. INTRODUCTION

Most recently charge excitations in stripe-ordered 214-type compounds $\text{La}_{5/3}\text{Sr}_{1/3}\text{NiO}_4$ and $\text{La}_{15/8}\text{Ba}_{1/8}\text{CuO}_4$ were studied using (indirect) resonant inelastic x-ray scattering (RIXS) by Wakimoto *et al.*¹ Excitations below and around 1-eV energy loss were observed with a momentum transfer \mathbf{q} corresponding to the charge stripe spatial period both for the nickelates and cuprates. This prominent \mathbf{q} dependence of the RIXS spectra has been interpreted by the authors as being due to collective stripe excitations or anomalous softening of the charge excitonic modes of the in-gap states. In what follows, we will offer a different interpretation of this outstanding \mathbf{q} dependence: The interference terms of the RIXS cross section produce a distinct directional dependence of the x-ray intensity re-emitted from a group of physically equivalent Ni/Cu atoms residing within the stripes. More generally speaking, the coherence of the absorption and re-emission process in RIXS gives rise to this interference phenomenon, which makes possible fluorescence interferometry (FI), as first described by Ma^{2,3} and interpreted by Ma and Blume⁴ in terms of the Young double slit experiment.

Applying the principles of FI to RIXS adds a further element of selectivity to this spectroscopy, that is, in addition to element and symmetry selectivity, the selectivity with respect to the re-emission of those atoms of the same element, which are interacting and physically equivalent due to their position within the lattice. Such site selectivity considerably enlarges the information content of RIXS. It will be shown how the prominent \mathbf{q} dependence of certain parts of the RIXS spectra is produced by FI and yields additional insight into the long-range order of their re-emitting centers via a partial structure factor. The basic idea of applying FI to RIXS is similar to that of diffraction anomalous fine structure.⁵

The paper is organized as follows: In Sec. II we will derive the basics of FI as arising from indirect RIXS, by treating shakeup RIXS in the third-order perturbation scheme for crystalline matter. We will end up with a relation for the differential cross section, which describes the interference

of the RIXS radiation from a group of identical, equivalent, and interacting atoms in the shakeup part of the resonance scattering process. This expression is determined by the partial structure factor of this group of atoms. In Sec. III we shortly summarize the experimental results on charge excitations of $\text{La}_{5/3}\text{Sr}_{1/3}\text{NiO}_4$ (LSNO) obtained by Wakimoto *et al.*,¹ as far as they exhibit the stripe-related \mathbf{q} dependence. Then we present the FI based calculation of the \mathbf{q} -dependent relative intensities of the stripe-related charge excitations of LSNO, utilizing two different models of the stripe structure. Here, FI is used to find out the appropriate model for a proper description of the charge stripe structure of LSNO. In Sec. IV we discuss the results of Wakimoto *et al.*¹ presented for $\text{La}_{15/8}\text{Ba}_{1/8}\text{CuO}_4$ (LBCO) in a similar manner. In Sec. V we can conclude that the prominent \mathbf{q} dependence of the stripe related charge excitations in the stripe ordered 214 compounds can be traced back to FI, which enables the site selectivity in addition to the symmetry and element selectivity of RIXS.

II. BASICS OF FLUORESCENCE INTERFEROMETRY

Utilizing FI for interpreting the \mathbf{q} dependence of indirect RIXS spectra has to start with treating the double differential scattering cross section for shakeup (indirect) RIXS in third-order perturbation calculation as derived by Döring *et al.*⁶ As schematically depicted in Fig. 1 for the case of nickelates the intermediate state $|n\rangle$ with energy E_n of the RIXS process is characterized by an electron-hole pair with a hole in the Ni $1s$ -core level and an electron in a Ni $4p$ level. This pair, which can be considered as a virtual exciton, takes up the momentum of the incident photon and can Coulomb interact with the valence electron system via the Hamiltonian H_C . Thus an additional scattering process, a so-called shakeup process in the intermediate state, takes place, which leads to a charge excitation of the Ni $3d$ system and promotes the whole system into a different intermediate state $|m\rangle$ with energy E_m . If the virtual exciton recombines, the total energy loss $\hbar\omega = \hbar(\omega_1 - \omega_2)$ of the RIXS process and the momentum transfer $\hbar\mathbf{q} = \hbar(\mathbf{K}_1 - \mathbf{K}_2)$ is imparted to the excitation of

the Ni 3*d* valence electron system. It is converted from its ground state $|i\rangle$ with a hole in the conduction band, when treated in one-electron approximation, to the final state $|f\rangle$ with an electron in the conduction band. ω_1 , ω_2 and \mathbf{K}_1 , \mathbf{K}_2 are the frequency and the wave vector of the incident

and scattered photon field, respectively. H_C is treated as a perturbing Hamiltonian. Thus one ends up with the following expression for the double differential scattering cross section in one-electron approximation describing the shakeup part of the resonant scattering process:

$$\left(\frac{d^2\sigma}{d\Omega_2 d\hbar\omega_2}\right)_{\text{shakeup}} \sim r_0^2 \frac{\omega_2}{\omega_1} \sum_i \sum_f \left| \sum_{m,n} \frac{\langle f|b_2|m\rangle \langle m|H_C|n\rangle \langle n|b_1|i\rangle}{(E_n - E_i - \hbar\omega_1 - i\frac{\Gamma_n}{2})(E_m - E_i - \hbar\omega_1 - i\frac{\Gamma_m}{2})} \right|^2 \times \delta(E_f - E_i - \hbar\omega), \quad (1)$$

where $|i\rangle$, $|f\rangle$ are the initial and final single-particle states of the scattering electron system with energies E_i and E_f . $r_0 = e^2/mc^2$ is the classical electron radius. For an adequate handling of the resonance denominator of Eq. (1) we have introduced Γ_n and Γ_m , which describe the energy broadening of the resonance due to the finite lifetime of the intermediate states. The scattering operators are defined as $b_1 = \mathbf{e}_1 \cdot \mathbf{p} \exp(i\mathbf{K}_1 \cdot \mathbf{r})$ and $b_2 = \mathbf{e}_2^* \cdot \mathbf{p} \exp(-i\mathbf{K}_2 \cdot \mathbf{r})$ with the corresponding polarization unit vectors $\mathbf{e}_{1/2}$, the momentum operator \mathbf{p} , and the position operator \mathbf{r} of the electron (dipole approximation).

If one wants to utilize FI as discussed in Ref. 3 in connection with shakeup (indirect) RIXS on crystalline matter, one has to follow up the interferences of the resonant inelastically scattered radiation from those re-emitting atoms, which are physically indistinguishable; see Ref. 4. This means that they must be identical atoms on physically equivalent sites. Therefore we will make the following Bloch-type single-particle ansatz for the initial band state $|i\rangle$ with a hole in the 4*p*-type conduction bands, going with unoccupied 3*d* conduction and occupied 3*d* valence bands. Accordingly, the final band state $|f\rangle$ is represented by a hole in the 4*p*-type conduction bands

but going with an electron in the 3*d* conduction and a hole in the 3*d* valence bands:

$$|i\rangle = \exp(i\mathbf{k}_i \cdot \mathbf{r}) u_{n_i}(\mathbf{r}), \quad (2)$$

$$|f\rangle = \exp(i\mathbf{k}_f \cdot \mathbf{r}) u_{n_f}(\mathbf{r}), \quad (3)$$

where $n_{i,f}$ is the band index, $\mathbf{k}_{i,f}$ the Bloch wave vector, and $u_n(\mathbf{r})$ is a lattice periodic function. The intermediate states $|n\rangle$ and $|m\rangle$ exhibit a hole in the core state. Because the core wave functions are localized, they can be written in tight-binding approximation:

$$|n\rangle = \frac{1}{N^{1/2}} \sum_{\mathbf{R}} \exp[i\mathbf{k}_c \cdot (\mathbf{R} + \mathbf{d}_s^\alpha)] \Phi_{n_j, \alpha}(\mathbf{r} - \mathbf{R} - \mathbf{d}_s^\alpha), \quad (4)$$

$$|m\rangle = \frac{1}{N^{1/2}} \sum_{\mathbf{R}} \exp[i\mathbf{k}_c \cdot (\mathbf{R} + \mathbf{d}_s^\alpha)] \Phi_{m_j, \alpha}(\mathbf{r} - \mathbf{R} - \mathbf{d}_s^\alpha). \quad (5)$$

\mathbf{R} is a lattice translation vector, \mathbf{k}_c is a Bloch wave vector, \mathbf{d}_s^α designates a certain group α of identical and equivalent atoms labeled s within the elementary cell determined by \mathbf{R} . n_j and m_j are the core-level indices. N is the number of unit cells in the elementary volume. The sum over intermediate states $|n\rangle$ and $|m\rangle$ in Eq. (1) includes both a sum over \mathbf{d}_s^α and a sum over Bloch vectors \mathbf{k}_c . The energies E_n and E_m are essentially constants, independent of \mathbf{R} and \mathbf{k}_c , so that the sum over \mathbf{k}_c can be replaced by a sum over lattice sites \mathbf{R} using

$$\sum_{\mathbf{k}_c} \exp[i\mathbf{k}_c \cdot (\mathbf{R} - \mathbf{R}')] = N \delta_{\mathbf{R}, \mathbf{R}'}. \quad (6)$$

We insert Eqs. (2)–(5) into Eq. (1) to calculate the double differential cross section for a shakeup process at identical and equivalent atoms of group α . Here we (i) substitute $\mathbf{r} - \mathbf{R} - \mathbf{d}_s^\alpha = \mathbf{r}'$, (ii) make use of the lattice periodicity of $u(\mathbf{r})$, and (iii) assume that the spatial extent of the core wave function is small compared to the lattice spacing, so that $\exp(-i\mathbf{k}_i \cdot \mathbf{r}') \approx 1$ and $\exp(i\mathbf{k}_f \cdot \mathbf{r}') \approx 1$ in the expressions of the dipole matrix

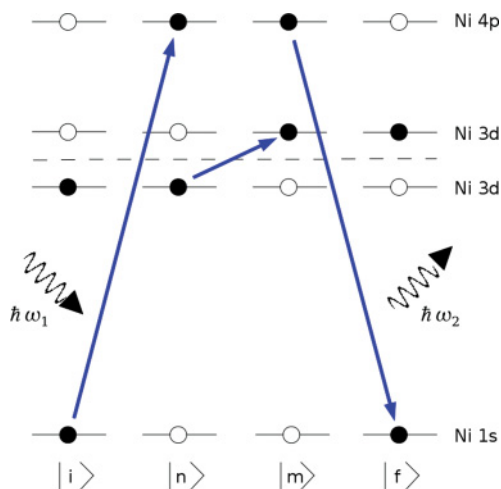


FIG. 1. (Color online) Scheme of an indirect RIXS process with shakeup excitation in the 3*d* electron system.

element of Eq. (1). Finally we end up with

$$\left(\frac{d^2\sigma}{d\Omega_2 d\hbar\omega_2}\right)_{\text{shakeup}}^\alpha \sim r_0^2 \frac{\omega_2}{\omega_1} \frac{1}{N^2} \sum_{n_i, \mathbf{k}_i} \sum_{n_f, \mathbf{k}_f} \left| \sum_{n_j, m_j} \frac{M_2(n_f, m_j, \alpha) M_C(n_j, m_j, \alpha) M_1(n_i, n_j, \alpha)}{(E_{n_i, \mathbf{k}_i} - E_{n_j, \alpha} - \hbar\omega_1 - i\frac{\Gamma_{n_j, \alpha}}{2})(E_{n_i, \mathbf{k}_i} - E_{m_j, \alpha} - \hbar\omega_1 - i\frac{\Gamma_{m_j, \alpha}}{2})} \right|^2 \times \sum_{\mathbf{R}, \mathbf{d}_s^\alpha} \exp[-i\mathbf{k}_i \cdot (\mathbf{R} + \mathbf{d}_s^\alpha)] \exp[i\mathbf{k}_f \cdot (\mathbf{R} + \mathbf{d}_s^\alpha)] \exp[i\mathbf{q} \cdot (\mathbf{R} + \mathbf{d}_s^\alpha)] \delta(E_{n_i, \mathbf{k}_i} - E_{n_f, \mathbf{k}_f} - \hbar\omega), \quad (7)$$

where the dipole matrix elements are

$$M_1(n_i, n_j, \alpha) = \int d\mathbf{r}' u_{n_i}(\mathbf{r}') \exp(i\mathbf{K}_1 \cdot \mathbf{r}') (\mathbf{e}_1 \cdot \mathbf{p}) \Phi_{n_j, \alpha}^*(\mathbf{r}'), \quad (8)$$

$$M_2(n_f, m_j, \alpha) = \int d\mathbf{r}' u_{n_f}(\mathbf{r}') \exp(-i\mathbf{K}_2 \cdot \mathbf{r}') (\mathbf{e}_2^* \cdot \mathbf{p}) \Phi_{m_j, \alpha}(\mathbf{r}'), \quad (9)$$

and

$$M_C(n_j, m_j, \alpha) \equiv \langle m | H_C | n \rangle. \quad (10)$$

Since M_1 , M_2 , M_C , $E_{n_j, \alpha}$, $\Gamma_{n_j, \alpha}$, $E_{m_j, \alpha}$, and $\Gamma_{m_j, \alpha}$ are independent of \mathbf{R} and \mathbf{d}_s^α , the sum over intermediate states in Eq. (7) can be carried out. Moreover, we integrate Eq. (1) with respect to ω obtaining the final expression for the differential cross section of a shakeup resonant inelastic scattering process (indirect RIXS), where the fluorescence radiation from identical and equivalent atoms of group α undergoes interferences:

$$\left(\frac{d\sigma}{d\Omega_2}\right)_{\text{shakeup}}^\alpha \sim r_0^2 \frac{\omega_2}{\omega_1} \frac{1}{N^2} \sum_{n_i, n_f} \left| \sum_{n_j, m_j} \frac{M_2(n_f, m_j, \alpha) M_C(n_j, m_j, \alpha) M_1(n_i, n_j, \alpha)}{(E_{n_f} - E_{n_j, \alpha} - \hbar\omega_2 - i\frac{\Gamma_{n_j, \alpha}}{2})(E_{n_f} - E_{m_j, \alpha} - \hbar\omega_2 - i\frac{\Gamma_{m_j, \alpha}}{2})} \right|^2 \times \sum_{\mathbf{k}_i, \mathbf{k}_f} N \delta(\mathbf{k}_f - \mathbf{k}_i + \mathbf{q}, \mathbf{g}) |F_\alpha(\mathbf{k}_f - \mathbf{k}_i + \mathbf{q})|^2 \equiv C(n_i, n_f, n_j, m_j, \alpha) I_{\text{rel}}, \quad (11)$$

where \mathbf{g} is an appropriate reciprocal-lattice vector. We have replaced E_{n_f, \mathbf{k}_f} in the denominators of Eq. (11) by E_{n_f} , the average of E_{n_f, \mathbf{k}_f} over \mathbf{k}_f , which is justified as long as Γ_{n_j, m_j} are comparable with the energy width of the n_f bands. This is the case for the nickelates and especially for the cuprates. In Eq. (11) we have introduced

$$F_\alpha(\mathbf{k}_f - \mathbf{k}_i + \mathbf{q}) \equiv \sum_{\mathbf{d}_s^\alpha} \exp[i(\mathbf{k}_f - \mathbf{k}_i + \mathbf{q}) \cdot \mathbf{d}_s^\alpha], \quad (12)$$

the partial structure factor related to the group α of identical and equivalent atoms labeled s in the elementary cell, and we have detached the relative intensity defined by

$$I_{\text{rel}} \equiv N^{-1} \sum_{\mathbf{k}_i, \mathbf{k}_f} |F_\alpha(\mathbf{k}_f - \mathbf{k}_i + \mathbf{g}_0 + \mathbf{q}^*)|^2 \times \delta(\mathbf{k}_f - \mathbf{k}_i + \mathbf{g}_0 + \mathbf{q}^*, \mathbf{g}) \quad (13)$$

from the expression of the scattering cross section. For a given structure of a group α of identical and equivalent atoms within the elementary cell I_{rel} is proportional to the integrated intensity of the re-emitted radiation as a function of momentum transfer \mathbf{q} , here represented as $\mathbf{q} = \mathbf{g}_0 + \mathbf{q}^*$ (\mathbf{g}_0 reduces \mathbf{q} into the first Brillouin zone and \mathbf{q}^* is the reduced momentum transfer vector).

In each case a certain range of \mathbf{k}_i 's within the \mathbf{g}_0 Brillouin zone defines an appropriate reciprocal-lattice vector \mathbf{g}' , so that one has to sum over these \mathbf{g}' when calculating I_{rel} according to

$$I_{\text{rel}} \equiv I_{\text{calc}} = \sum_{\mathbf{g}'} G(\mathbf{g}', \mathbf{q}) |F_\alpha(\mathbf{g}')|^2, \quad (14)$$

with weight factors

$$G(\mathbf{g}', \mathbf{q}) = \frac{1}{N} \sum_{\mathbf{k}_i, \mathbf{k}_f} \delta(\mathbf{k}_f - \mathbf{k}_i + \mathbf{g}_0 + \mathbf{q}^*, \mathbf{g}'). \quad (15)$$

III. CHARGE EXCITATIONS IN $\text{La}_{5/3}\text{Sr}_{1/3}\text{NiO}_4$

In their studies on LSNO Wakimoto *et al.*¹ have found that the integrated intensity I_{exp} of the indirect RIXS spectra between 0.35- and 0.65-eV energy loss is strongly \mathbf{q} dependent (see Table I and Fig. 2 showing RIXS spectra exemplarily for two extreme cases) with a distinct maximum at $\mathbf{q}_{\text{ab}} = \mathbf{q}_s = (1/a)(4\pi/3, 2\pi/3)$, a momentum transfer corresponding to the diagonal charge stripe spatial period of $(3a/2, 3a/2)$,⁷ as depicted in Fig. 3.

This \mathbf{q} dependence has been interpreted in Ref. 1 to be due to collective stripe excitations or anomalous softening of the charge excitonic modes of the in-gap states.

In what follows, we want to demonstrate that the application of the principles of FI as given in Eqs. (11)–(15) will lead to an alternative interpretation: Here, this \mathbf{q} dependence is

TABLE I. Experimental relative integral intensity of RIXS structures between 0.35- and 0.65-eV energy loss of $\text{La}_{5/3}\text{Sr}_{1/3}\text{NiO}_4$ compared to calculated values for two different stripe models S1 and S2. (1) indicates units of $(1/a, 1/b)$ (2D elementary cell); (2) indicates units of $(2\pi/3a, 2\pi/3b, 2\pi/2c)$ (supercell). Intensities are given in arbitrary units (see text).

$\mathbf{q}_{ab}^{(1)}$	$\frac{\Theta}{2} [^\circ]$	$\mathbf{q}^{(2)}$	$\mathbf{g}_0^{(2)}$	I_{exp}	$I_{\text{calc}}^{\text{S1}}$	$I_{\text{calc}}^{\text{S2}}$
$(2\pi, 0)$	44.72	$(3, 0, 23.1)$	$(3, 0, 24)$	16.5 ± 2	11.8	11.76
$(\frac{3\pi}{2}, 0)$	45.15	$(2.25, 0, 23.68)$	$(2, 0, 24)$	20.1 ± 2	3.13	0.79
$(\pi, 0)$	45.41	$(1.5, 0, 24.08)$	$(1, 0, 24)$	16.9 ± 2	3.2	3.2
$(\pi, \frac{\pi}{2})$	45.07	$(1.5, 0.75, 23.9)$	$(1, 1, 24)$	15.1 ± 2	19.28	19.28
(π, π)	45.02	$(1.5, 1.5, 23.7)$	$(1, 2, 24)$	12.3 ± 2	25.29	25.29
$(\frac{4\pi}{3}, \frac{2\pi}{3})$	44.67	$(2, 1, 23.5)$	$(2, 1, 24)$	35.2 ± 2	35.2	13.86
$(\frac{3\pi}{2}, \frac{\pi}{2})$	44.81	$(2.25, 0.75, 23.5)$	$(2, 1, 24)$	24.4 ± 2	23.93	7.11

a direct consequence of interferences in the fluorescence radiation emitted within the RIXS process by Ni^{3+} ions, which constitute, according to a stripe model of Yamamoto *et al.*,⁸ the centers of the hole stripes, shown in Fig. 3.

Within the limits of this stripe model, the $d-d$ charge excitations of these Ni^{3+} ions in an energy-loss range of 1 eV should be different from those of the Ni^{2+} ions. The projected density of states calculated in Ref. 8 shows clearly that, contrary to the Ni^{2+} site, the position of $x^2 - y^2$ orbitals on the Ni^{3+} site shifts to the energy region just above the Fermi energy thus opening a gap. Across this gap $d-d$ charge excitations can occur that are not present at the Ni^{2+} site, where the position of the $x^2 - y^2$ orbitals remains below the Fermi energy. This way the Ni^{3+} ions play the role of identical and equivalent centers of FI related RIXS, as introduced in Sec. II. We will treat at first a stripe model in which the position of the Ni^{3+} ions are defined within a $3a \times 3b \times 2c$ supercell shown for the corresponding four NiO_2 layers in Fig. 3 as follows in units of $a = b = 3.81495 \text{ \AA}$, $c = 12.6849 \text{ \AA}$:⁹ first layer $(0, 0, 0)$, $(1, 1, 0)$, and $(2, 2, 0)$; second layer $(0.5, 2.5, 0.5)$, $(1.5, 0.5, 0.5)$, and $(2.5, 1.5, 0.5)$; third layer (stripe rotation by

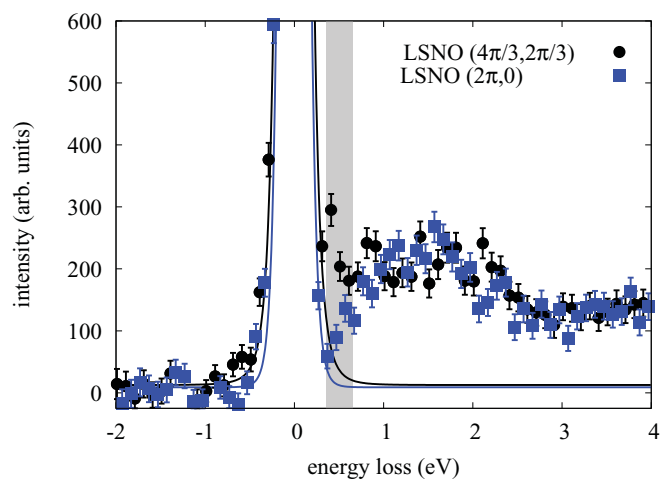


FIG. 2. (Color online) Indirect RIXS spectra of $\text{La}_{5/3}\text{Sr}_{1/3}\text{NiO}_4$ for momentum transfer with $\mathbf{q}_{ab} = (2\pi, 0)$ and $\mathbf{q}_{ab} = \mathbf{q}_s = (4\pi/3, 2\pi/3)$. The corresponding fits of the quasielastic line are shown as solid lines and the integration range of experimental data is shaded (see text for details). Data by courtesy of Wakimoto *et al.*¹

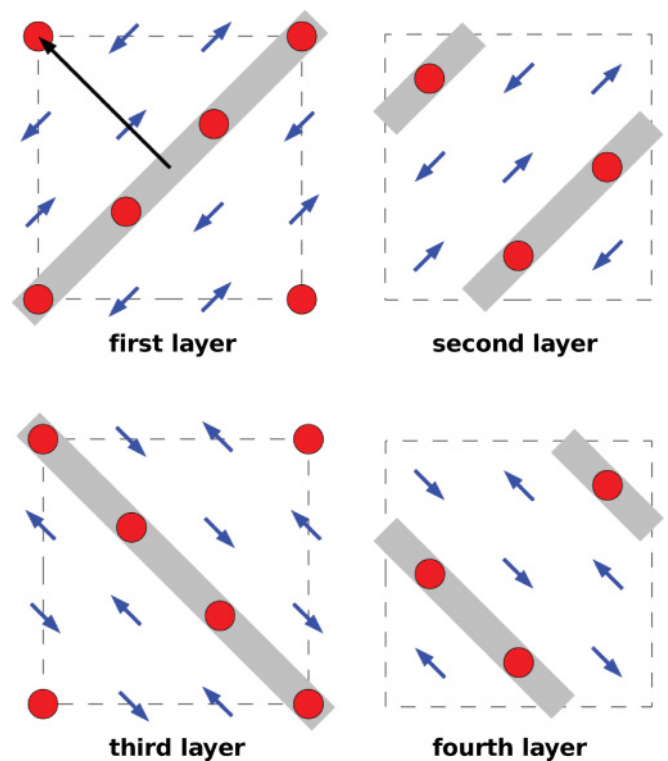


FIG. 3. (Color online) Diagonal charge stripes of $\text{La}_{5/3}\text{Sr}_{1/3}\text{NiO}_4$ in the basal (ab) NiO_2 plane (first layer), in the second, third, and fourth NiO_2 plane at a distance from the basal plane of $c/2$, c , and $3c/2$, respectively. The third and fourth layers show orthogonal stripe orientation. Only Ni atoms are represented. Charge stripes are marked as shaded belts. The filled circles indicate the hole carrying Ni (Ni^{3+}). The black arrow shows the spatial period of the stripes. The broken lines are the boundaries of the $3a \times 3b \times 2c$ supercell. This representation corresponds to the stripe model 1 with staggered position of the stripes between the first and second as well as third and fourth layers.

90°) $(0, 3, 1)$, $(1, 2, 1)$, and $(2, 1, 1)$; fourth layer $(0.5, 1.5, 1.5)$, $(1.5, 0.5, 1.5)$, and $(2.5, 2.5, 1.5)$. This way we have chosen, as proposed by Tranquada,⁷ a staggered configuration of the stripes between the first and second layers, as also between the third and fourth layers. In addition we have introduced domains with mutually perpendicular stripe orientation (due to tetragonal symmetry), which might have long-range order within the ab plane (correlation lengths are up to 400 \AA ; see Ref. 9). In contrast, according to Ref. 9, the correlation length in the c direction is about 15 \AA , which is close to the value of the c lattice parameter. Therefore to simplify matters, we have chosen the domain size in the c direction to be uniform equal to c . A real distribution of domain sizes in the c direction will not affect qualitatively the results of our calculation provided that the average domain size is not far above the value of 15 \AA . This stripe model guarantees an equal population of both types of stripe domains. A second stripe model we have treated is based on a nonstaggered configuration with the following Ni^{3+} positions: first layer $(0, 0, 0)$, $(1, 1, 0)$, and $(2, 2, 0)$; second layer $(0.5, 0.5, 0.5)$, $(1.5, 1.5, 0.5)$, and $(2.5, 2.5, 0.5)$; third layer $(0, 3, 1)$, $(1, 2, 1)$, and $(2, 1, 1)$; fourth layer $(0.5, 2.5, 1.5)$, $(1.5, 1.5, 1.5)$, and $(2.5, 0.5, 1.5)$. These Ni^{3+} coordinates were

introduced into Eqs. (14) and (15) using the momenta of the measurements (see Table I). The momentum components in the ab plane are given by the authors of Ref. 1, the component with respect to the c plane can be calculated from the experimental scattering angles.¹⁰ The reciprocal-lattice vectors are related to the $3a \times 3b \times 2c$ supercell. Both the relative sample orientation in the experiment (estimated from the anisotropy of the \mathbf{q} resolution in Ref. 1) and the solid angle of the scattered beam accepted by the analyzer (0.0064 sr) have been taken into account. The relative intensities I_{rel} of radiation re-emitted from the Ni^{3+} ions as calculated are scaled to the arbitrary units of the intensity I_{exp} of the RIXS spectra integrated between 0.35 and 0.65 eV taken from Ref. 1 in such a way that they agree at $\mathbf{q}_s = (1/a)(4\pi/3, 2\pi/3)$ for the first stripe model. The contribution of the quasielastic line, which was determined by a fit to the experimental data between -2.2 and 0.2 eV using a Pearson function, was subtracted to give a proper estimate for I_{exp} .

The comparison between calculation and experiment is summarized in Table I and depicted in Fig. 4. The calculations on the basis of the first stripe model (staggered) are in qualitative agreement with the experiment. In particular it is the distinct peak of the integrated intensity for $\mathbf{q}_s = \mathbf{q}_{ab} = (1/a)(4\pi/3, 2\pi/3)$, which is well reproduced by the calculations. Thus it is demonstrated that FI offers an explanation of the unique \mathbf{q} dependence of the 0.35–0.65-eV charge excitations seen in the indirect RIXS spectra of LSNO. Remaining differences between experimental and calculated intensities, larger than the statistical errors, may be attributed to deficiencies of the stripe model used. We would like to note that the calculation using the second stripe model (nonstaggered) does not agree with the experimental data. Therefore FI allows us to distinguish between different structural models and provides a proof for the validity of the staggered stripe model.

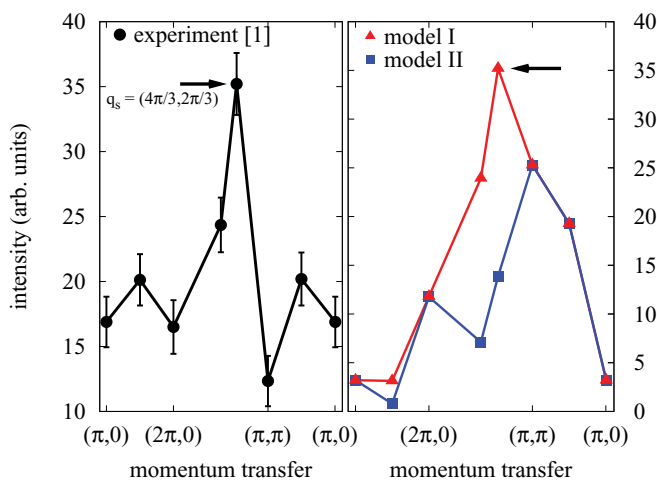


FIG. 4. (Color online) Momentum transfer dependence of the experimental RIXS intensity I_{exp} of $\text{La}_{5/3}\text{Sr}_{1/3}\text{NiO}_4$ integrated between 0.35- and 0.65-eV energy loss (circles) compared to the calculated FI-based intensity I_{rel} both for the stripe model 1 (staggered, triangles) and for stripe model 2 (nonstaggered, squares). The experimental intensity is scaled to agree with the calculated intensity of stripe model 1 at \mathbf{q}_s (marked by an arrow).

TABLE II. Experimental relative integral intensity of RIXS structures between 0.9- and 1.3-eV energy loss of $\text{La}_{15/8}\text{Ba}_{1/8}\text{CuO}_4$ compared to calculated values of the stripe and the kink model. (1) indicates units of $(1/a, 1/b)$ (2D elementary cell); (2) indicates units of $(2\pi/8a, 2\pi/8b, 2\pi/2c)$ (supercell). Intensities are given in arbitrary units (see text).

$\mathbf{q}_{ab}^{(1)}$	$\frac{\Theta}{2} [^\circ]$	$\mathbf{q}^{(2)}$	$\mathbf{g}_0^{(2)}$	I_{exp}	$I_{\text{calc}}^{\text{S}}$	$I_{\text{calc}}^{\text{kink}}$
(π, π)	45.64	(4,4,27)	(4,4,27)	0.20 ± 0.01	0.27	0.18
$(\pi, \frac{\pi}{2})$	45.28	(4,2,27)	(4,2,27)	0.25 ± 0.01	0.17	0.19
$(\pi, 0)$	45.16	(4,0,27)	(4,0,27)	0.35 ± 0.01	0.30	0.27
$(\frac{\pi}{2}, 0)$	44.80	(2,0,27)	(2,0,27)	0.46 ± 0.01	0.99	0.46
(0,0)	44.68	(0,0,27)	(0,0,27)	0.33 ± 0.01	0.26	0.27
$(\frac{\pi}{2}, \frac{\pi}{2})$	44.92	(2,2,27)	(2,2,27)	0.35 ± 0.01	0.00	0.15

This is a unique application of FI yielding interesting structural information by making RIXS site selective.

IV. CHARGE EXCITATIONS IN $\text{La}_{15/8}\text{Ba}_{1/8}\text{CuO}_4$

Similarly to LSNO, for LBCO the integral intensity I_{exp} of the indirect RIXS spectra between 0.9- and 1.3-eV energy loss is strongly \mathbf{q} dependent,¹ which is summarized in Table II and shown in Fig. 5.

I_{exp} has a distinct maximum at $\mathbf{q}_{ab} = \mathbf{q}_s = (1/a)(\pi/2, 0)$, a momentum transfer corresponding to the parallel charge stripe spatial period of $(4a, 0)$, as depicted in Fig. 6. This \mathbf{q} dependence has been interpreted to be due to collective stripe excitations.¹ However, as discussed for LSNO, the LBCO \mathbf{q} dependence can be interpreted also as a direct consequence of interferences in the fluorescence radiation emitted within the RIXS process. Here the interferences are due to fluorescence emission from Cu atoms at the nonmagnetic domain walls, which separate the antiferromagnetic domains according to the stripe model treated by Fleck *et al.*¹¹ (see Fig. 6).

These authors have shown, within the limits of their calculations using dynamical mean-field theory (see Fig. 8

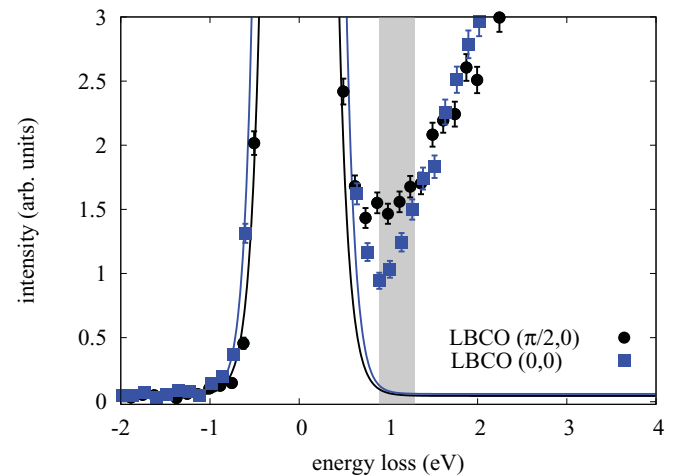


FIG. 5. (Color online) Indirect RIXS spectra of $\text{La}_{15/8}\text{Ba}_{1/8}\text{CuO}_4$ for $\mathbf{q}_{ab} = \mathbf{q}_s = (\pi/2, 0)$ (symbols) and $\mathbf{q}_{ab} = (0, 0)$ (symbols). The contribution of the quasielastic lines obtained by a fit are shown as solid lines and the integration range of experimental data is shaded (see text). Data by courtesy of Wakimoto *et al.*¹

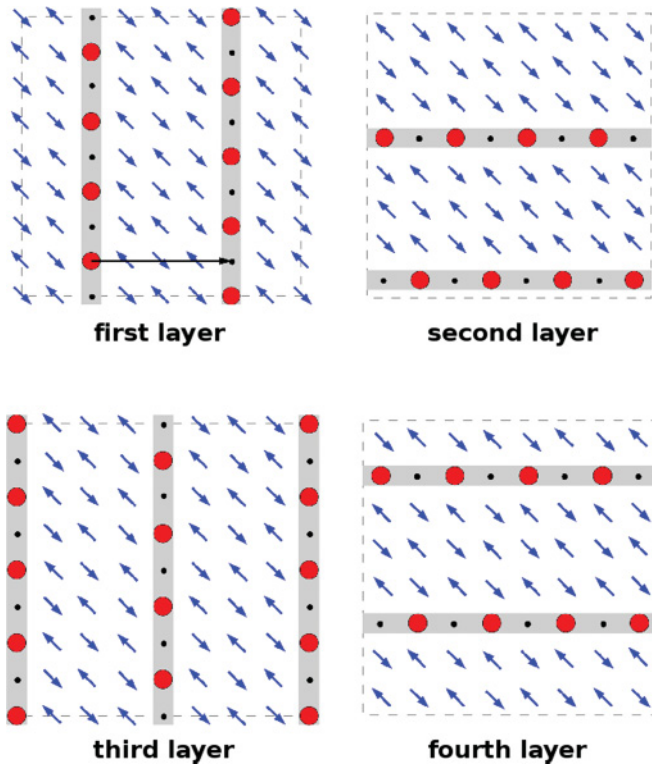


FIG. 6. (Color online) Parallel charge stripes of $\text{La}_{15/8}\text{Ba}_{1/8}\text{CuO}_4$ in the basal (ab) CuO_2 plane (first layer) and next three CuO_2 planes at a distance of $c/2$ from each other. Only Cu atoms are represented. Charge stripes are marked as shaded belts. The filled circles indicate the hole carrying Cu atoms. The black arrow shows the spatial period of the stripes. The broken lines are the boundaries of the $8a \times 8b \times 2c$ supercell.

in Ref. 11), that there are distinct differences between the imaginary part of the local self-energy for atoms at the domain wall and for the first and second neighbors of the domain wall. Especially in the vicinity of the chemical potential a pseudogap is opened (see Fig. 12 in Ref. 11). Its width is smaller for the domain-wall atoms than for the domain-wall neighbors. Thus the d - d charge excitations across this gap should be of the order of 1 eV or less for the domain-wall atoms, and of the order of 2 eV or more for the domain-wall neighbors. This way the Cu atoms at the domain wall play the role of identical and equivalent centers for FI related RIXS re-emission. We will treat FI for indirect RIXS spectra of LBCO using the stripe model depicted in Fig. 6 for the supercell in the four CuO_2 layers. The position of the stripes in the first two layers has been proposed by Traquada *et al.*⁷ In this model the stripes are rotated by 90° from layer to layer in order to follow the structural modulation associated with the tilting of the CuO_6 octahedra. Holes are located at the antiphase domain boundaries. A filled circle denotes the presence of one hole, centered on a metal site. For our calculations we have assumed ordering of the holes. Only metal sites with a hole are considered as identical and equivalent centers of FI related RIXS emission. The offset of the charge order by $2a$ between successive unit cells, which appears in the third and fourth layers of this stripe model, has been claimed by Abbamonte *et al.*¹² on account of their

resonant soft x-ray scattering studies on LBCO. We will refer to this model, in what follows, as the stripe model. We have extended our FI calculation to a modification of this stripe model by introducing kinks along the domain wall within the $8a \times 8b \times 2c$ supercell, as discussed by Fleck *et al.*¹¹ Such a structure is shown exemplarily for one layer in Fig. 7. The kinks were assumed to be randomly distributed with 1.5 kinks along a domain-wall section of length $8a$. We will refer, in what follows, to this modified model as the kink model.

The coordinates of the hole carrying Cu atoms were introduced into Eqs. (14) and (15) using the experimental momentum transfers (see Table II). Their components in the ab plane are given in Ref. 1, the c component is calculated from the experimental scattering angles as discussed before.¹⁰ The reciprocal-lattice vectors used are related to the $8a \times 8b \times 2c$ supercell, as depicted in Fig. 6, with $a = b = 3.788 \text{ \AA}$ and $c = 13.23 \text{ \AA}$ taken from Ref. 12. Both the relative sample orientation of the experiment,¹ estimated from the anisotropy of the \mathbf{q} resolution, and the solid angle of the scattered beam accepted by the analyzer (0.0040 sr) have been taken into account. The relative intensities I_{rel} of radiation emitted from the hole carrying Cu atoms as calculated are scaled to the arbitrary units of the experimental intensity I_{exp} of the RIXS spectra integrated between 0.9- and 1.3-eV energy loss in such a way that they agree at $\mathbf{q}_s = (1/a)(\pi/2, 0)$ with results from the kink model. Here the quasielastic line was fitted in the energy-loss range between -2.2 and 0.4 eV and subtracted from the experimental data before integration. The well pronounced peak of the intensity curve as a function of \mathbf{q} as well as its width provides information on how the distribution of the hole carrying Cu atoms, i.e., the charge stripe structure, is reflected by the FI result. The obtained intensity values of calculation and experiment are summarized in Table II and depicted in Fig. 8. The calculations on the basis of the first stripe model exhibit the most important feature of the experiment, i.e., the strong peak of the integrated intensity at \mathbf{q}_s . Already this observation demonstrates that FI offers an explanation of the \mathbf{q} dependence of the charge excitations between 0.9 and 1.3 eV seen in the indirect RIXS spectra of LBCO. Even better agreement between calculations and experiment is found for the kink model. Not only the peak position of the calculated intensity curve as a function of \mathbf{q} but also its width agrees with

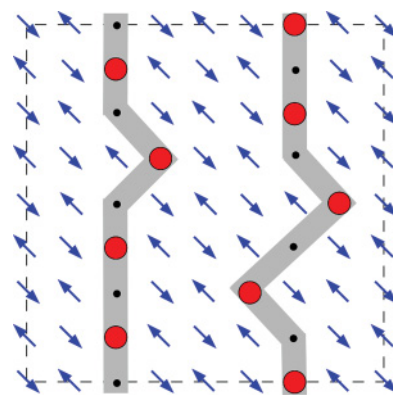


FIG. 7. (Color online) Parallel charge stripes of $\text{La}_{15/8}\text{Ba}_{1/8}\text{CuO}_4$ in the basal (ab) CuO_2 plane, here plotted exemplarily for the kink model. Symbols as for Fig. 6.

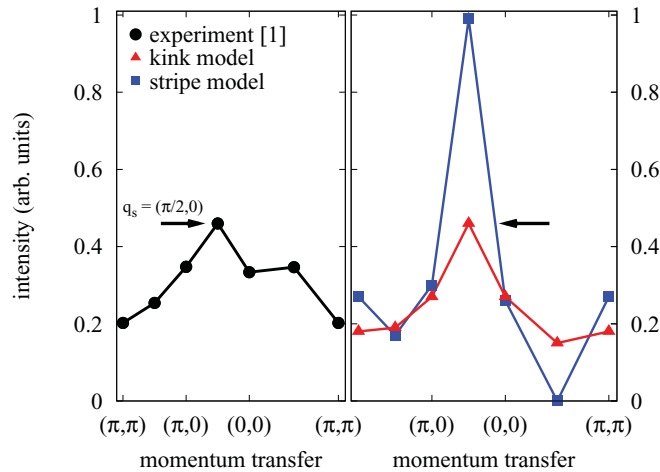


FIG. 8. (Color online) Momentum transfer dependence of the experimental RIXS intensity I_{exp} of $\text{La}_{15/8}\text{Ba}_{1/8}\text{CuO}_4$ integrated between 0.9- and 1.3-eV energy loss (circles, error bars are within the point size) compared to the calculated FI-based intensity I_{rel} both for the stripe model (squares) and for the kink model (triangles). The experimental intensity is scaled to agree with the calculated intensity of the kink model at \mathbf{q}_s (marked by an arrow).

the experimental results. This can be regarded as a hint that kinks along the domain walls, with a density as assumed in these calculations, must be considered as intrinsic features of the stripe structure of the 214-type cuprates.

V. CONCLUSIONS

It has been shown that applying the principles of FI to the interpret indirect RIXS spectral structures in stripe ordered 214-type nickelates and cuprates can explain their unique \mathbf{q} dependence. It is the interference of fluorescence radiation emitted in the RIXS process by hole carrying Ni/Cu atoms residing in the charge stripes, which leads to a strong enhancement of emitted intensity for momentum transfers \mathbf{q} corresponding to the charge stripe spatial periods. Moreover, a careful analysis of the \mathbf{q} dependence of the integrated RIXS intensity from the group of hole carrying Ni/Cu atoms enables information about details of the charge stripe structure. These applications of FI were founded on the derivation of the interference pattern in terms of the fundamentals of indirect RIXS. In particular, using the principles of FI for interpretation of RIXS spectra the site selectivity of RIXS can be employed, which yields interesting information supplementary to the well-known element and symmetry selectivity of RIXS.

ACKNOWLEDGMENTS

The authors thank the group of S. Wakimoto for making available to us the indirect RIXS data of their experiments on the 214-type nickelates and cuprates. Especially we thank K. Ishii for valuable discussions. We acknowledge M. Tolan for support.

¹S. Wakimoto, H. Kimura, K. Ishii, K. Ikeuchi, T. Adachi, M. Fujita, K. Kakurat, Y. Koike, J. Mizuki, Y. Noda, K. Yamada, A. H. Said, and Yu. Shvyd'ko, *Phys. Rev. Lett.* **102**, 157001 (2009).

²Y. Ma, *Phys. Rev. B* **49**, 5799 (1994).

³Y. Ma, *Chem. Phys. Lett.* **230**, 451 (1994).

⁴Y. Ma and M. Blume, *Rev. Sci. Instrum.* **66**, 1543 (1995).

⁵H. Stragier, J. O. Cross, J. J. Rehr, L. B. Sorensen, C. E. Bouldin, and J. C. Woicik, *Phys. Rev. Lett.* **69**, 3064 (1992).

⁶G. Döring, C. Sternemann, A. Kaprolat, A. Mattila, K. Hämäläinen, and W. Schülke, *Phys. Rev. B* **70**, 085115 (2004).

⁷J. M. Tranquada, *Ferroelectrics* **177**, 43 (1996).

⁸S. Yamamoto, T. Fujiwara, and Y. Hatsugai, *Phys. Rev. B* **76**, 165114 (2007).

⁹G. Wu, J. J. Neumeier, Ch. D. Ling, and D. N. Argyriou, *Phys. Rev. B* **65**, 174113 (2002).

¹⁰K. Ishii (private communication).

¹¹M. Fleck, A. I. Lichtenstein, and A. M. Oles, *Phys. Rev. B* **64**, 134528 (2001).

¹²P. Abbamonte, A. Rusydi, S. Smadici, G. D. Gu, G. A. Sawatzky, and D. L. Feng, *Nat. Phys.* **1**, 155 (2005).